Supplementary Information (SI) for Journal of Materials Chemistry A.
This journal is © The Royal Society of Chemistry 2024

Supporting Information

Mechanisms of oxygen transport resistance for mesoporous carbon supported catalysts in fuel cells

Kai-Bo An, Wen-Zhen Fang*, Zi-Hao Xuan, Guo-Rui Zhao, Han Ling, Wen-Quan Tao

Key Laboratory of Thermo-Fluid Science and Engineering of MOE, School of Energy and Power Engineering, Xi'an Jiaotong University, Xi'an, Shaanxi 710049, China

* Corresponding author: Wen-Zhen Fang, fangwenzhen@xjtu.edu.cn

S1 Theoretical model of oxygen transport in interior pores

The diffusion equation in the pore is determined as follows:

$$\frac{dJ_{O_2}^{int}(y)}{dy}+\frac{j_{int}(y)}{4F}=0 \qquad \text{* MERGEFORMAT (1)}$$

where $J_{O_2}^{int}(y)$ is the through pore flux of O_2, calculated by Eq. * MERGEFORMAT (2); $j_{int}(y)$ is the current density at the any space point *y* and *F* is Faraday's constant.

$$J_{O_2}^{int}(y)=-D_{O_2,H_2O}\frac{dc_{O_2}^{int}(y)}{dy} \qquad \text{* MERGEFORMAT (2)}$$

where D_{O_2,H_2O} is the diffusion coefficient of O_2 in water and $c_{O_2}^{int}(y)$ is the oxygen concentration in the pore at the any space point *y*, the concentration also continuously decreases, as shown in Fig. 1(f). The source term can be calculated by Eq. * MERGEFORMAT (3) [1,2].

$$\frac{j_p(y)}{4F}=\left(\frac{a_{ECSA}^{int}m_{Pt}^{int}}{h_P}\right)\frac{1}{R_{ads}^{H_2O}}\left[c_{O_2}^{int}(y)-c_{O_2,Pt}(y)\right] \qquad \text{* MERGEFORMAT (3)}$$

Where $R_{ads}^{H_2O}$ is the adsorption resistance at water/Pt interface; h_P is the pore depth; $c_{O_2,Pt}(y)$ is the oxygen concentration on the Pt surface at the any space point *y*; a_{ECSA}^{int} is the electrochemical specific area (ECSA) of interior Pt particles and m_{Pt}^{int} is the Pt loading of a pore, calculated by Eq. * MERGEFORMAT (4).

$$m_{Pt}^{int}=f_{Pt}^{int}\rho_C f_a h_P/\varepsilon_P(1-f_a) \qquad \text{* MERGEFORMAT (4)}$$

$$f_a=m_{Pt}/(m_C+m_{Pt}) \qquad \text{* MERGEFORMAT (5)}$$

where m_C is the mass of the carbon support. Therefore the O_2 concentration equation can be determined by

$$\frac{d^2c_{O_2}^{int}(y)}{dy^2}=\frac{a_{ECSA}^{int}m_{Pt}^{int}}{D_{O_2,H_2O}h_P R_{ads}^{H_2O}}c_{O_2}^{int}(y)=\frac{1}{\psi^2}c_{O_2}^{int}(y) \qquad \text{* MERGEFORMAT (6)}$$

$$\psi=\sqrt{D_{O_2,H_2O}h_P R_{ads}^{H_2O}\Big/a_{ECSA}^{int}m_{Pt}^{int}} \qquad \text{* MERGEFORMAT (7)}$$

The following boundary conditions are assigned for solving Eq. * MERGEFORMAT (6):

(I) Boundary condition for inlet concentration:

$$c_{O_2}^{int}\left(h_P\right)=c_{H_2O}^{int} \qquad \text{* MERGEFORMAT (8)}$$

where $c_{H_2O}^{int}$ is the O_2 concentration at the water film side of the gas/water interface.

(II) Boundary condition for bottom flux:

$$J_{O_2}^{int}\left(0\right)=0 \qquad \text{* MERGEFORMAT (9)}$$

Thus, the Eq. * MERGEFORMAT (6) can be solved and the O_2 concentration in the pore can be deduced:

$$c_{O_2}^{int}(y)=\frac{c_{H_2O}^{int}}{\cosh\left(\frac{h_P}{\psi}\right)}\cosh\left(\frac{y}{\psi}\right) \qquad \text{* MERGEFORMAT (10)}$$

Combining Eq. * MERGEFORMAT (2) and * MERGEFORMAT (10), the O_2 flux within the pore can be obtained:

$$J_{O_2}^{int}\left(y\right)=-D_{O_2,H_2O}\frac{dc_{O_2}^{int}(y)}{dy}=-D_{O_2,H_2O}\frac{c_{H_2O}^{int}}{\cosh\left(\frac{h_P}{\psi}\right)}\frac{1}{\psi}\sinh\left(\frac{y}{\psi}\right) \qquad \text{* MERGEFORMAT (11)}$$

S2 MD simulation details

In this study, the potential energy of all molecules in the model is expressed by the COMPASSIII [3] (Condensed-phase Optimized Molecular Potentials for Atomistic Simulation Studies) force field as

$$
\begin{aligned}
E = & \sum_{bond}\left[K_{b2}(b-b_o)^2 + K_{b3}(b-b_o)^3 + K_{b4}(b-b_o)^4\right] \\
& + \sum_{angle}\left[K_{a2}(\theta-\theta_o)^2 + K_{a3}(\theta-\theta_o)^3 + K_{a4}(\theta-\theta_o)^4\right] \\
& + \sum_{trosion}\left[K_{t1}(1-\cos\varphi) + K_{t2}(1-\cos 2\varphi) + K_{t3}(1-\cos 3\varphi)\right] \\
& + \sum_{OOPA} K_{\chi}(\chi-\chi_0)^2 + \sum_{bond/bond} K_{bb}(b-b_0)(b'-b'_0) \\
& + \sum_{bond/angle} K_{ba}(b-b_0)(\theta-\theta_o) + \sum_{angle/angls} K_{aa}(\theta-\theta_o)(\theta'-\theta'_o) \\
& + \sum_{bond/torsion}(b-b_0)\left[K_{bt1}\cos\varphi + K_{bt2}\cos 2\varphi + K_{bt3}\cos 3\varphi\right] \\
& + \sum_{angls/torsion}(\theta-\theta_o)\left[K_{at1}\cos\varphi + K_{at2}\cos 2\varphi + K_{at3}\cos 3\varphi\right] \\
& + \sum_{angle/trosion/angle} K(\theta-\theta_o)(\theta'-\theta'_o)(\varphi-\varphi_o) \\
& + \sum_{i>j}\frac{q_i q_j}{r_{ij}} + \sum_{i>j} E_{ij}\left[2\left(\frac{r_{ij}^0}{r_{ij}}\right)^9 - 3\left(\frac{r_{ij}^0}{r_{ij}}\right)^6\right]
\end{aligned}
\quad \backslash* \text{MERGEFORMAT (12)}
$$

$$
r_{ij}^0 = \left(\frac{\left(r_i^0\right)^6 + \left(r_j^0\right)^6}{2}\right)^{1/6} \qquad \backslash* \text{MERGEFORMAT (13)}
$$

The first ten terms in Eq. * MERGEFORMAT (12) represent the sum of energy changes caused by bond stretching, angle bending, and dihedral angle variations, including diagonal and off-diagonal cross coupling terms. The eleventh term is the Coulombic term for electrostatic interactions, and the twelfth term is the Lennard-Jones potential describing van der Waals interactions.

The investigation of oxygen permeation depends heavily on the diffusion coefficient, which is directly proportional to the slope of the linear portion of the mean square displacement (*MSD*) curve. The diffusion coefficient *D* can be calculated from the *MSD* obtained through MS[4]:

$$
D = \frac{1}{6N}\lim_{\Delta t\to\infty}\frac{1}{\Delta t}\left[\sum_{i=1}^{N}\left(\vec{r}_i(t+\Delta t) - \vec{r}_i(t)\right)^2\right] \qquad \backslash* \text{MERGEFORMAT (14)}
$$

where the subscript *i* represents the diffusion atoms, $\vec{r}_i$ is the central position vector, *N* is the total number of diffusing atoms, and *t* is the simulation time.

The partition coefficient *K* is calculated using the Henry constant K_H:

$$K = \frac{1}{K_H RT} \qquad \text{* MERGEFORMAT (15)}$$

where R is the gas constant, and T is the temperature.

The K_H is obtained using the "Sorption" module in the MS. 10^6 inserting tests are performed for each configuration using the Widom particle insertion method to represent the ensemble average[5]. The final K_H is achieved by averaging the values of 100 configurations.

S3 Model validation

To validate the rationality of the model, the density of the existing ionomer model is compared with experimental and simulated data in the reference, as shown in Fig. S1(a). Due to the constraints of experimental, only a Nafion thick film with a thickness of 100 μm could be used, which cannot achieve the nanoscale of Pt surface ionomers. As a result, there are some differences between the simulation results and the experimental results. It can be observed that as the λ of the ionomer increases, the density gradually decreases from 1.98 g·cm^{-3} to 1.71 g·cm^{-3}, which is generally consistent with the reference values[6–8]. Subsequently, the diffusion coefficient and partition coefficient of oxygen in the ionomer at 353 K are calculated, as shown in Fig. S1(b)-(c). The simulation results for the diffusion coefficient and partition coefficient closely match Kudo's experimental[9] findings and are consistent with Suzuki's[10] fitting curve, and both coefficients increase with increasing water content. Therefore, it can be considered that the model constructed and the parameters set in this study, and the simulation results are reliable.

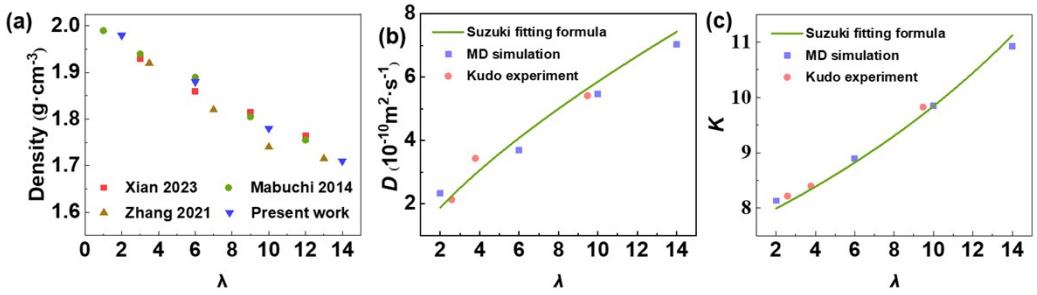

Figure S1. Comparison of molecular dynamics simulation data with experimental data (a) validation of polymer density, (b) validation of oxygen diffusion coefficient in the ionomer, (c) validation of oxygen partition coefficient with ionomer

S4 Resistance ratio and equivalent thickness

Although the transport resistances are all varied with λ, it is found that the contributions of R_{ads}, R_{dis} and R_{dif} are almost constant regardless of λ, accounting for 79%, 12%, 9%, respectively, as shown in Fig. S2(a). The equivalent thickness of interfacial resistances that include R_{ads} and R_{dis}, estimated by $\delta_e = (R_{dis} + R_{ads})/(R_{dif}/\delta_{ion})$, are within the range of 40 ~ 50 nm much higher than the typical thickness of ionomer films, as shown in Fig. S2(b), which has a good agreement with Kudo et al. [9] experimental data.

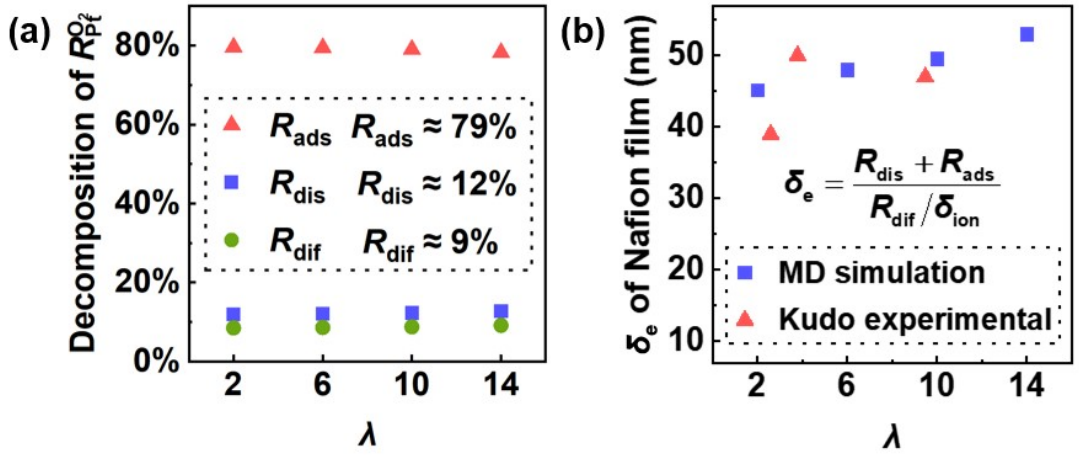

Figure S2. Oxygen transport resistances of ionomer-Pt catalysts. (a) Contributions of R_{ads}, R_{dis}, R_{dif} to $R_{Pt}^{O_2}$ with respect to λ; (b) The equivalent thickness of interfacial resistances and its comparison with Kudo et al. experimental data.

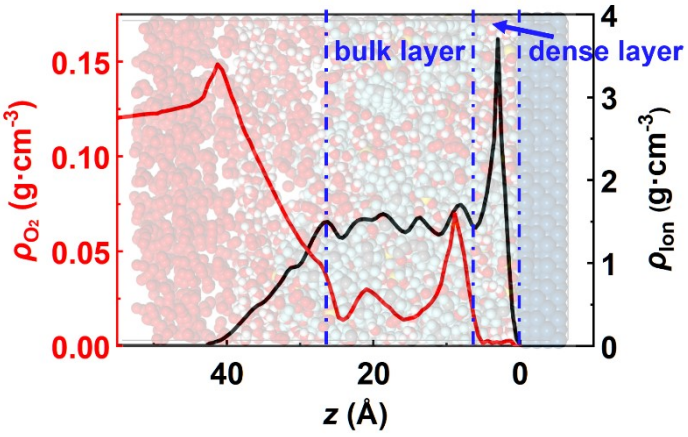

Figure S3 Density distributions of oxygen and ionomer in the thickness direction

S5 Verification of adsorption resistance

The interior pore resistance was estimated through experimental data[11], followed by iterative refinement using the bisection method until the resistance calculated by Eq. 10 matched that determined experimentally. The required R_{ads} were thus obtained.

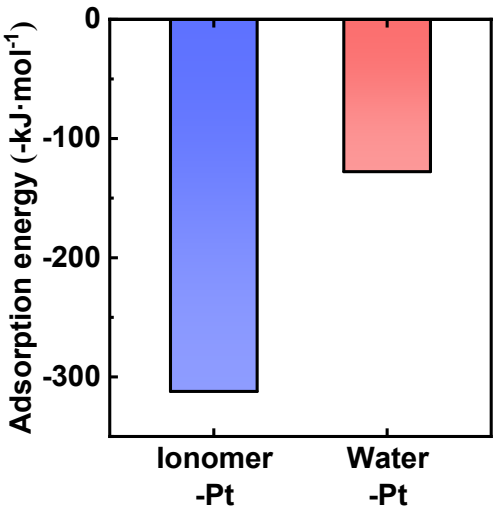

Figure S4. The variation in adsorption energy of Ionomer-Pt and Water-Pt.

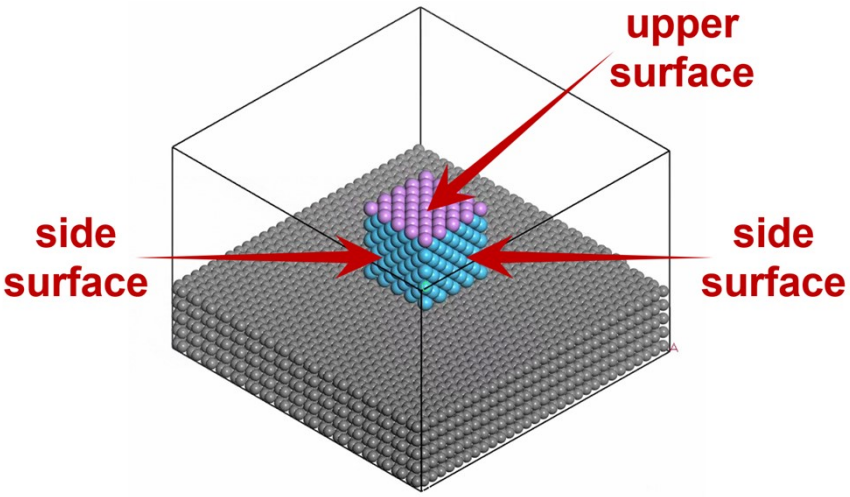

Figure S5. Schematic diagram of the upper surface and side surface (the purple part is the upper surface, and the blue part is the side surface).

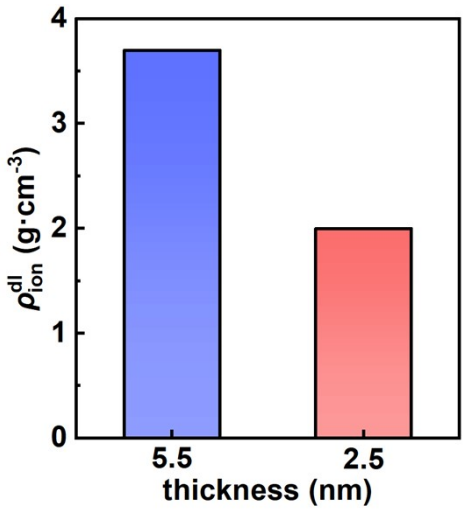

Figure S6. Density comparison of ionomers at 2.5nm and 5.5nm.

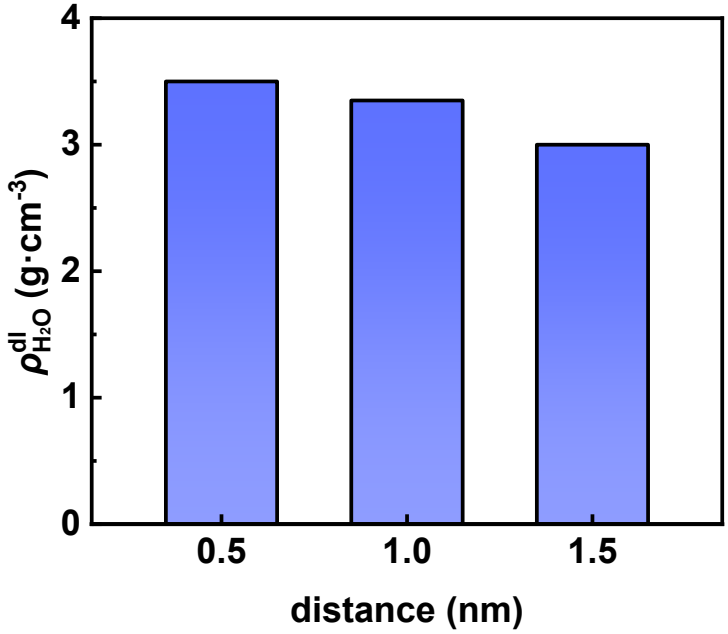

Figure S7. Density comparison of the dense layer between the two Pt nanoparticles.

S6 Fitting process of diffusion coefficient formula

The Arrhenius equation [12] is commonly used to describe the relationship between temperature and diffusion coefficient, expressed as:

$$D = D_0 \exp\left(-\frac{E_a}{RT}\right) \qquad \text{* MERGEFORMAT (16)}$$

Where D_0 represents the pre-exponential factor, E_a represents the diffusion activation energy, R is the gas constant, and T is the temperature. Plotting the reciprocal of temperature against the

logarithm of the diffusion coefficient in Fig. S8, a proper fitting yields the diffusion activation energy of oxygen at different λ with a determination coefficient R^2 for the fits ranging from 0.9902~0.9998. After performance, the fitting yields:

$$E_a = 32.5538 - 2.5783\lambda^{0.5} \quad \text{* MERGEFORMAT (17)}$$

Of which the determination coefficient R^2 is at a sensible value of 0.9982, indicating that the fitted equation for the diffusion activation energy as a function of water content is reliable. Since oxygen diffusion within the ionomer film varies with λ, different diffusion behaviors can be characterized. Therefore, the fitted equation for D_0 can also be obtained from Fig. S8:

$$D_0 = 0.0897\lambda^{-0.2087} - 0.0336 \quad \text{* MERGEFORMAT (18)}$$

The determination coefficient R^2=0.9999 indicates excellent fit. Consequently, the overall fitted equation for the oxygen diffusion coefficient within the ionomer membrane can be derived:

$$D = \left(0.0897\lambda^{-0.2087} - 0.0336\right)\exp\left(-\frac{32.5538 - 2.5783\lambda^{0.5}}{RT}\right) \text{* MERGEFORMAT (19)}$$

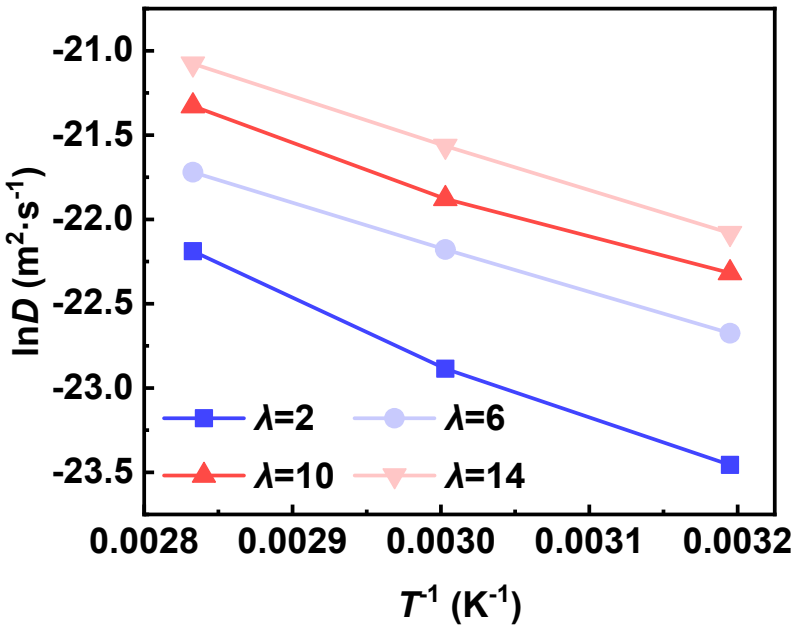

Figure S8. The relationship between diffusion coefficient and temperature.

References

1 T. A. Greszler, D. Caulk and P. Sinha, *J. Electrochem. Soc.*, 2012, **159**, F831–F840.

2 T. Schuler, A. Chowdhury, A. T. Freiberg, B. Sneed, F. B. Spingler, M. C. Tucker, K. L. More, C. J. Radke and A. Z. Weber, *J. Electrochem. Soc.*, 2019, **166**, F3020–F3031.

3 H. Sun, *J. Phys. Chem. B*, 1998, **102**, 7338–7364.

4 K. An, Z. Wang, X. Yang, Z. Qu, F. Sun, W. Zhou and H. Zhao, *Journal of Environmental Chemical Engineering*, 2022, **10**, 108723.

5 S. Ban, C. Huang, X.-Z. Yuan and H. Wang, *J. Phys. Chem. C*, 2012, **116**, 17424–17430.

6 T. Mabuchi and T. Tokumasu, *The Journal of Chemical Physics*, 2014, **141**, 104904.

7 L. Xian, Z. Li, S. Li, L. Chen and W.-Q. Tao, *International Journal of Heat and Mass Transfer*, 2023, **208**, 124034.

8 G. Zhang, G. Yang, S. Li, Q. Shen, H. Wang, Z. Li, Y. Zhou and W. Ye, *Membranes*, 2021, **11**, 695.

9 K. Kudo, R. Jinnouchi and Y. Morimoto, *Electrochimica Acta*, 2016, **209**, 682–690.

10 T. Suzuki, K. Kudo and Y. Morimoto, *Journal of Power Sources*, 2013, **222**, 379–389.

11 V. Yarlagadda, M. K. Carpenter, T. E. Moylan, R. S. Kukreja, R. Koestner, W. Gu, L. Thompson and A. Kongkanand, *ACS Energy Lett.*, 2018, **3**, 618–621.

12 Y. Ma, X. Liu, X. Zhou, Y. He, J. Tang, F. Su, W. Yang, S. Fan, J. Wang, Z. Li and J. Yang, *Chemical Engineering Journal*, 2023, **451**, 138535.